

Measurements of diffractive structure functions with the LRG method and using the leading proton spectrometer at ZEUS

Jaroslav Lukasik *

DESY/AGH-UST Cracow
Notkestrasse 85, D-22607 Hamburg - Germany

The ZEUS detector has been used to study dissociation of virtual photons, $\gamma^* p \rightarrow Xp$, in e^+p collisions at HERA in events with a large rapidity gap (LRG) between X and the outgoing proton, as well as in events with a measured leading proton. The data cover photon virtualities $Q^2 > 2 \text{ GeV}^2$, with $M_X > 2 \text{ GeV}$, where M_X is the mass of the hadronic final state X . The results are presented in terms of the diffractive structure functions, $F_2^{D(3)}$ and $F_2^{D(4)}$.

1 Introduction

The diagram of the diffractive Deep Inelastic ep Scattering (DIS) is shown in the Fig. 1. This process is characterised by the fact that p loses a small fraction of its energy and emerges from the scattering intact or dissociated into a low-mass state with a transverse momentum squared typically much smaller than 1 GeV^2 . The diffractive DIS events can be described, in addition to standard DIS variables, by the four-momentum transfer at p vertex squared t and invariant mass of γ^*P system M_X which is the mass of the system resulting from virtual photon dissociation. If also proton dissociates into higher mass state it will be denoted by N . Moreover, the diffractive structure functions are often expressed in terms of x_P and β variables. In a model with Pomeron exchange in the t channel x_P is the fraction of the proton momentum carried by the Pomeron, while β corresponds to the momentum fraction of the struck quark within the Pomeron.

The ZEUS collaboration used two different experimental approaches to select the inclusive diffractive events:

- measurement of the final state proton by means of a Leading Proton Spectrometer (LPS method) [2],
- a large rapidity gap in the forward direction requirement (LRG method).

The preliminary results obtained with the LPS and LRG methods will be presented in the following.

The data used for this measurement were taken with the ZEUS detector at HERA ep collider in the year 2000, where HERA collided positrons of 27.6 GeV with protons of 920 GeV. The data used for the LRG and LPS analyses correspond to integrated luminosities of 45.4 pb^{-1} and 32.6 pb^{-1} , respectively. The results presented here cover photon virtualities $Q^2 > 2 \text{ GeV}^2$, photon-proton centre-of-mass energies $40 < W < 240 \text{ GeV}$ and proton

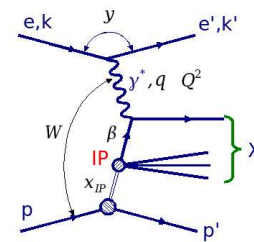


Figure 1: Diagram of the diffractive Deep Inelastic ep Scattering.

*On behalf of the ZEUS Collaboration.

fractional momentum losses $0.0002 < x_{\mathcal{P}} < 0.02$ (LRG sample) or $0.0002 < x_{\mathcal{P}} < 0.1$ (LPS sample).

1.1 LPS method

In most of the diffractive events outgoing proton stays intact and provides a clean experimental signature. Since p_t of the outgoing proton is expected to be small (less than 1 GeV typically), it escapes through the forward beam hole. A fraction of these events can be detected by the Leading Proton Spectrometer (LPS). In the spectrum of protons measured in the LPS shown as a function of $x_L = |p_f|/|p_i|$, where p_i and p_f are the initial and final proton momenta respectively [4], a characteristic peak is observed at $x_L \simeq 1$ which corresponds to photon diffractive dissociation events. A clean sample of diffractive events is obtained by requiring $x_L > 0.97$. Measurement of the scattered proton four-momentum allows to study the t distribution in inclusive diffractive dissociation.

1.2 LRG method

Experimental determination of the rapidity gap rely on calculation of the pseudorapidity of the most forward going particle η_{max} , which deposits some minimum amount of energy (above noise level) in the detector.

The η_{max} distribution in the DIS sample is characterised by a plateau like structure, due to diffractive events mainly, which extends to a low η_{max} values (large $\Delta\eta$). By setting an upper limit on the maximum pseudorapidity (e.g. $\eta_{max} < 3$), a diffractive sample with relatively low non-diffractive background can be selected.

2 Results

The data are presented in terms of the diffractive structure functions, $F_2^{D(3)}$ and $F_2^{D(4)}$. The results can be also presented in terms of the reduced cross section [3], $\sigma_r^{D(3)}(x_{\mathcal{P}}$, which is equal to the conventional $F_2^{D(3)}$ up to corrections due to the longitudinal structure function.

The contributions from longitudinal structure function F_L^D and Z_0 exchanges have been neglected in presented results.

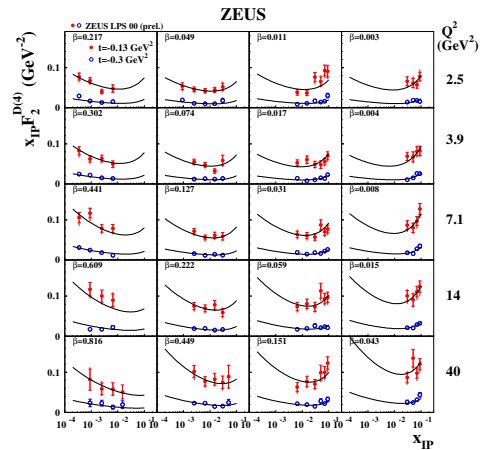


Figure 2: The diffractive structure function multiplied by $x_{\mathcal{P}}$, $x_{\mathcal{P}} F_2^{D(4)}$, in two t bins as a function of $x_{\mathcal{P}}$ for different values of Q^2 and β . The normalisation uncertainty of 10% is not shown. The continuous lines are the result of the Regge fit described in the text.

2.1 Results from the LPS method

Figure 2^a shows the measured structure function $x_{\mathcal{P}}F_2^{D(4)}$. For $x_{\mathcal{P}} < 0.01$ the structure function rises with decreasing $x_{\mathcal{P}}$. For higher values of $x_{\mathcal{P}}$ it starts to rise with increasing $x_{\mathcal{P}}$. This latter effect is attributed to the contributions from Regge trajectory exchanges regge-exch.

A sum of two contributions was fitted to the data according to

$$F_2^{D(4)} = f_{\mathcal{P}}(x_{\mathcal{P}}, t) \cdot F_2^{\mathcal{P}}(\beta, Q^2) + n_{\mathcal{R}} \cdot f_{\mathcal{R}}(x_{\mathcal{P}}, t) \cdot F_2^{\mathcal{R}}(\beta, Q^2).$$

The first term of this sum is the contribution from Pomeron exchange and the second one, from the exchanges of the Reggeon trajectories. The Reggeon structure function $F_2^{\mathcal{R}}(\beta, Q^2)$ was taken to be equal to the pion structure function as parametrised by GRV [5]. The fit was limited to $y < 0.5$ to reduce the influence of F_L^D . Result of the fit is shown in the Fig. 2.

2.2 Results from the LRG method

Inclusive diffractive data were selected with LRG method by requiring the maximum pseudorapidity to be $\eta_{max} < 3$ outside the Forward Plug Calorimeter (FPC) [7]. In addition events with energies in the FPC larger than 1 GeV were rejected.

The resulting diffractive structure function $x_{\mathcal{P}}F_2^{D(3)}$ is shown in Figures 3-5. The result of a Regge fit, performed in the same way as described previously, is shown as the continuous lines. It gives a good description of the data. No rise of $x_{\mathcal{P}}F_2^{D(3)}$ coming from Regge-exchanges can be seen because the LRG data end essentially at $x_{\mathcal{P}} = 0.01$.

The ratio of the $F_2^{D(3)}$ values obtained with the LPS method to the LRG data is shown in Fig. 6 up to $Q^2 = 40 \text{ GeV}^2$. The ratio is independent of $x_{\mathcal{P}}$ and equal in each β and Q^2 bin with the average value $0.82 \pm 0.01(stat) \pm 0.03(syst)$. Since up to $x_{\mathcal{P}} = 0.01$ the LPS data contain no contribution from proton dissociation, this is an indication that the contribution from proton dissociation in the LRG data might be about 18%. However, one has to take into account the large normalisation uncertainty of about 10% of the LPS data.

3 Bibliography

References

- [1] Slides: <http://indico.cern.ch/contributionDisplay.py?contribId=61&sessionId=7&confId=9499>
- [2] ZEUS Coll., M. Derrick *et al.*, Z. Phys. **C73** 253 (1997).
- [3] H1 Coll., A. Aktas *et al.*, hep-ex/0606004.
- [4] ZEUS Coll., J. Breitweg *et al.*, Eur. Phys. J. **C1** 81 (1998).
- [5] M. Glück, E. Reya and A. Vogt, Z. Phys. **C53** 127 (1992);
M. Glück, E. Reya and A. Vogt, Z. Phys. **C53** 651 (1992);
M. Glück, E. Reya and A. Vogt, Z. Phys. **C67** 433 (1995).
- [6] P. D. B. Collins, *An Introduction to Regge Theory and High Energy Physics*, Cambridge University Press, Cambridge (1977).
- [7] ZEUS Coll., FPC group, A. Bamberger *et al.*, Nucl. Inst. Meth. **A450** 235 (2000).

^aFrom now on in each plot the inner error bars will indicate the statistical uncertainties, the outer bars the statistical and systematic uncertainties summed in quadrature.

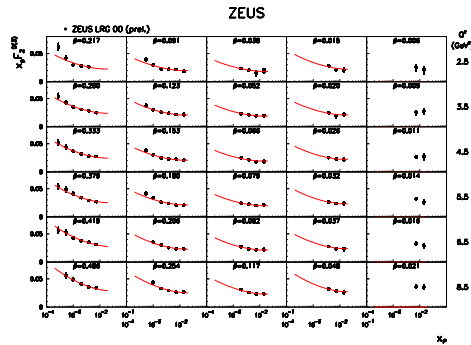


Figure 3: The diffractive structure function multiplied by $x_{\mathbb{P}}, x_{\mathbb{P}}F_2^{D(3)}$, obtained with the LRG method as a function of $x_{\mathbb{P}}$ for different values of Q^2 and β at low Q^2 values. The normalisation uncertainty of $\pm 2.25\%$ is not shown. The continuous lines are the result of the Regge fit described in the text.

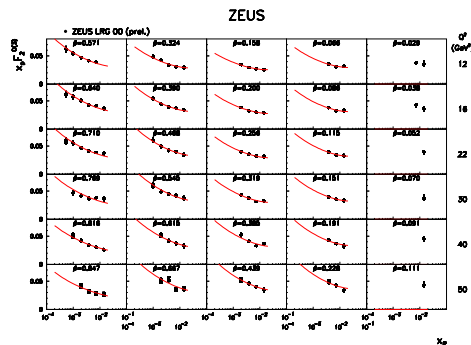


Figure 4: The diffractive structure function multiplied by $x_{\mathbb{P}}, x_{\mathbb{P}}F_2^{D(3)}$, obtained with the LRG method as a function of $x_{\mathbb{P}}$ for different values of Q^2 and β at intermediate Q^2 values. The normalisation uncertainty of $\pm 2.25\%$ is not shown. The continuous lines are the result of the Regge fit described in the text.

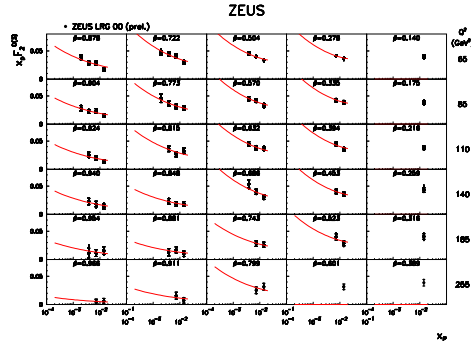


Figure 5: The diffractive structure function multiplied by $x_{\mathcal{P}}$, $x_{\mathcal{P}} F_2^{D(3)}$, obtained with the LRG method as a function of $x_{\mathcal{P}}$ for different values of Q^2 and β at high Q^2 values. The normalisation uncertainty of $\pm 2.25\%$ is not shown. The continuous lines are the result of the Regge fit described in the text.

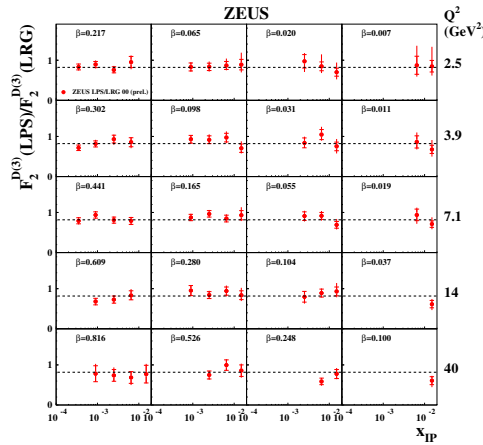


Figure 6: The ratio of the structure functions $F_2^{D(3)}$ as obtained with the LPS and LRG methods as a function of $x_{\mathcal{P}}$ for different values of Q^2 and β . The normalisation uncertainty of ${}_{-10}^{+12}\%$ is not shown. The lines indicate the average value of the ratio.